The propagation of high-Reynolds-number non-Boussinesq gravity currents in axisymmetric geometry

M A R I U S   U N G A R I S H†

Department of Computer Science, Technion, Haifa 32000, Israel

We consider the propagation of a non-Boussinesq gravity current in an axisymmetric configuration (full cylinder or wedge). The current of density ρ_c is released from rest from a lock of radius r_0 and height h_0 into an ambient fluid of density ρ_a in a container of height H. When the Reynolds number is large, the resulting flow is governed by the parameters ρ_c/ρ_a and $H^* = H/h_0$. We show that the one-layer shallow-water model, carefully combined with a Benjamin-type front condition, provides a versatile formulation for the thickness and speed of the current, without any adjustable constants. The results cover in a continuous manner the range of light $\rho_c/\rho_a \ll 1$, Boussinesq $\rho_c/\rho_a \approx 1$, and heavy $\rho_c/\rho_a \gg 1$ currents in a fairly wide range of depth ratio, H^*. We obtain finite-difference solutions for the propagation and show that a self-similar behaviour develops for large times. This reveals the main features, in particular: (*a*) The heavy current propagates faster and its front is thinner than that for the light counterpart; (*b*) For large time, *t*, both the heavy and light currents spread like $t^{1/2}$, but the thickness profiles display significant differences; (*c*) The energy-constrained propagation with the thickness of half-ambient-depth (when H^* is close to 1) is a very limited occurrence, in contrast to the rectangular geometry counterpart in which this effect plays a major role. The predictions of the simple model are supported by some axisymmetric Navier–Stokes finite-difference simulations.

Key words: axisymmetric, bare spot, gravity current, Navier Stokes, non-Boussinesq, self-similar, shallow water

1. Introduction

We consider the propagation of a gravity current of density ρ_c into an ambient fluid of density ρ_a in a container of height H. The geometry is cylindrical and the propagation is in the positive radial direction over (or beneath) a horizontal wall. When $\rho_c/\rho_a > 1$, we refer to a heavy (dense, bottom) current, and when $\rho_c/\rho_a < 1$ we refer to a light (ceiling, top) current. (Note that the light or heavy term is with respect to the ambient.) The current is released from a lock (of radius r_0 and height h_0) adjacent to the horizontal boundary on which it will spread out. The configuration is illustrated in figure 1. We assume that the Reynolds number $Re = u_{ref} h_0/\nu$ is large and hence viscous effects can be discarded (here u_{ref} is the typical speed of the current and ν is the representative kinematic viscosity of the fluids). The flow can be

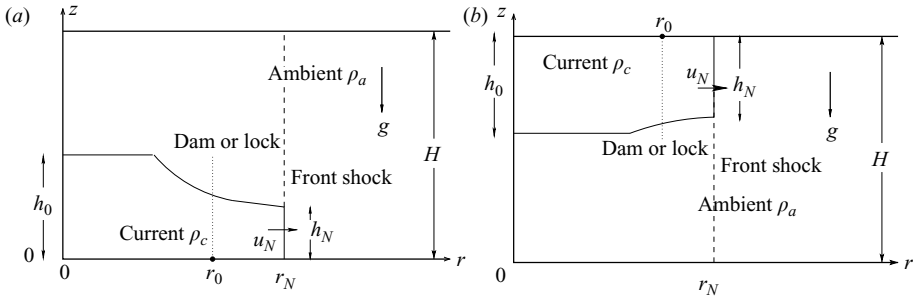† Email address for correspondence: unga@cs.technion.ac.il

FIGURE 1. Schematic description of the (*a*) heavy and (*b*) light currents released from a cylinder lock of radius r_0 and height h_0 into an ambient of height H.

considered axisymmetric in both a full cylinder and a wedge (assuming a sufficiently large opening angle).

It is well known that in the Boussinesq case $\rho_c/\rho_a \approx 1$, the light and heavy currents display the same behaviour. To be specific, in the configuration of figure 1, the bottom and top Boussinesq currents would appear as mirror images with respect to the horizontal boundary (but note that our figure emphasized the lack of symmetry). The Boussinesq currents depend on one parameter only, the depth ratio

$$H^* = H/h_0, \tag{1.1}$$

which can be in the range $[1, \infty)$. This does not make it an easy problem in general, but after many years of investigation there is a solid body of knowledge and well-developed prediction tools for this current; this is illustrated and discussed by Ungarish (2007*a*, 2009).

The non-Boussinesq flow is more complicated. First, there is the mathematical difficulty introduced by the fact that the propagation depends on an additional parameter, the density ratio ρ_c/ρ_a, which theoretically is in the range $(0, \infty)$. (We exclude from our direct analysis the special $\rho_a = 0$ case of a liquid propagating freely into a gas or vacuum). Second, the setup of experiments and simulations with fluids of significantly different densities requires more resources than the relatively simple (like water-saline) systems used for the Boussinesq cases. For these reasons, laboratory experiments and Navier–Stokes simulations of non-Boussinesq currents are scarce even for the two-dimensional (rectangular) geometry, and practically non-existent for the axisymmetric case.

The investigations of the two-dimensional non-Boussinesq currents clearly demonstrate that the Boussinesq symmetry for light–heavy currents disappears when ρ_c/ρ_a departs from 1, and that the non-Boussinesq effects are important in both the initial (slumping) and the developed (self-similar) stages; see (Ungarish 2007*b*, hereafter referred to as U) and the references therein. Valuable insights into the observed behaviour and useful predictions of the speed of propagation were obtained by shallow-water (SW) models (Lowe, Rottman & Linden 2005; U). The extension of these results to the axisymmetric geometry is a non-trivial task that requires dedicated studies. An attempt in this direction is presented here.

The analytical model presented by Lowe, Rottman & Linden (2005) (following Keller & Chyou 1991) uses a two-layer SW formulation. The solution, which was derived for a full-depth lock exchange, $H^* = 1$, considers only the slumping

stage during which the vertical fronts (shocks) move with constant speed. In the cylindrical geometry, the matching conditions for the interface (which are an essential component in that solution) are complicated by curvature terms, and the constant speed assumption is, in general, not valid. In view of these additional analytical difficulties, and the restriction to $H^* = 1$, the extension of the Lowe *et al.* (2005) model to the axisymmetric problem was not pursued here. The model of U uses a one-layer SW formulation. It has been applied to various lock-depth release, $H^* \geqslant 1$, and covers in a continuous manner the slumping, intermediate and self-similar stages of propagation. The major advantage of this model is the mathematical simplicity that allows for a continuous coverage of the full (H^*, ρ_c/ρ_a) parameters domain (the Boussinesq current is now a narrow strip about $\rho_c/\rho_a = 1$ in this domain). U showed good agreement with available data, and more recent numerical simulations provide further support to the applicability of this model to a wide range of parameters (Bonometti, Balachandar & Magnaudet 2008; Bonometti & Balachandar 2009). It makes sense to attempt an extension of this model for the current that propagates in a cylindrical geometry. An inspection reveals that the main assumptions can be carried over, and the additional curvature terms do not complicate significantly the mathematical formulation (although they may complicate or defy analytical solutions). More importantly, the resulting equations are expected to reproduce continuously the initial, intermediate and long-time phases, until viscous forces become important.

We wish to emphasize that a versatile theoretical model for the axisymmetric current is of practical importance. Various applications to environmental, industrial and hazard-prediction problems are concerned with radial-cylindrical gravity currents. One could hope to fill the gap of knowledge with Navier–Stokes (NS) simulations. However, even for Boussinesq cases, the axisymmetric numerical codes for the NS equations reveal an instability that renders, eventually, unphysical flow fields. There is evidence that these simulations disagree with experimental observations after the current has spread out to $r_N \approx 2.5$–3, scaled with r_0; see Patterson *et al.* (2006) and Ungarish (2007*a*). The full three-dimensional simulations overcome this difficulty (the problematic axisymmetric instability is dissipated by the three-dimensional motion) but a typical run requires weeks of CPU time on powerful computers (Cantero, Balachandar & Garcia 2007). On the other hand, the SW Boussinesq axisymmetric model is not subject to that instability and provides fairly accurate predictions for larger r_N than the NS axisymmetric simulations (see Ungarish 2007*a*). We expect that these properties carry over to the non-Boussinesq problems.

The foregoing considerations provide the motivation for the present study. The objective is to investigate the propagation of the axisymmetric non-Boussinesq gravity current using, mainly, an extension of the one-layer SW model. This is expected to point out, in simple terms, the major differences between the 'light' and 'heavy' currents and between the axisymmetric and two-dimensional non-Boussinesq counterparts. Moreover, the resulting model is expected to be a useful (approximate but very fast) prediction tool for the whole range of light, Boussinesq and heavy inviscid currents.

The structure of the paper is as follows. The SW model is formulated in §2. The main results are presented in §3: finite-difference solutions of the SW equations for the release-from-rest problem, the tendency to self-similar propagation (which can be expressed analytically) and some comparisons with NS simulations. These results point out the differences between the light and heavy currents and illustrate the prediction capabilities of the simple SW model. Some concluding remarks are given in §4.

2. Formulation

We consider incompressible, immiscible fluids, and assume that the viscous effects are negligible (both in the interior and at the boundaries). The density of the current and the ambient is ρ_c and ρ_a, respectively. The typical flow is conveniently described in a cylindrical system, and we assume axial symmetry and no swirl (azimuthal) velocity component. The current propagates into the positive r direction, and the gravitational acceleration g acts into the negative z direction. The bottom and the top of the container are at $z = 0$ and $z = H$. The propagating fluid is originally in a reservoir of radius r_0 and height h_0 located adjacent to the boundary on which propagation occurs, i.e. the bottom for the heavy current and the top for the light current; see figure 1.

We use dimensional variables unless stated otherwise. The thickness of the current is $h(r, t)$ and its horizontal velocity (z-averaged) is $u(r, t)$. Initially, at $t = 0$, $h = h_0$ and $u = 0$. We assume a shallow current that is relevant for $h_0/r_0 \ll 1$.

The continuity equation is

$$\frac{\partial h}{\partial t} + u \frac{\partial h}{\partial r} + h \frac{\partial u}{\partial r} = -\frac{uh}{r}. \tag{2.1}$$

The momentum balances are used below. Let p denote the pressure reduced with $+\rho_a g z$, and the subscripts a, c denote the ambient and the current domains. The SW approximation shows that in the z direction the pressure obeys the hydrostatic balance for both a and c fluids. The one-layer model also argues that the r-momentum flux of the return flow in the ambient is, in many cases of interest, negligible (compared with that of the current) and hence $p_a = C$. Consequently, pressure continuity $p_c = p_a$ at the interface ($z = h(r, t)$ for the heavy current, and $z = H - h(r, t)$ for the light) yields

$$p_c(r, z, t) = -\Delta \rho g z + |\Delta \rho| g h(r, t) + C_1, \tag{2.2}$$

where $\Delta \rho = \rho_c - \rho_a$, and $C_1 = C$ and $C + \Delta \rho H$ for the heavy and light currents, respectively. Finally, the z-averaged r-momentum equation is employed for the c fluid to express the balance between the inertial forces (proportional to ρ_c) and the $-\partial p_c/\partial r$ term, which is eliminated by (2.2). We assume that the deviation of the real horizontal velocity component from the z-averaged u is small, which is a reasonable approximation for low-viscosity fluids released from rest. We obtain

$$\frac{\partial u}{\partial t} + u \frac{\partial u}{\partial r} = -\frac{|\Delta \rho|}{\rho_c} g \frac{\partial h}{\partial r}. \tag{2.3}$$

The system (2.1) and (2.3) for $h(r, t)$ and $u(r, t)$ is hyperbolic, and the characteristic equations can be expressed as

$$\left(\frac{|\Delta \rho|}{\rho_c} g \right)^{1/2} \mathrm{d}h \pm h^{1/2} \, \mathrm{d}u = \mp \left(\frac{|\Delta \rho|}{\rho_c} g \right)^{1/2} \frac{uh}{r} \, \mathrm{d}t \tag{2.4}$$

on

$$\frac{\mathrm{d}r}{\mathrm{d}t} = u \pm \left(\frac{|\Delta \rho|}{\rho_c} g \right)^{1/2} h^{1/2}. \tag{2.5}$$

For obtaining realistic gravity current solutions, the system of equations must be subjected to a boundary condition at the nose (or front) $r = r_N(t)$; see Ungarish (2009) for a discussion. The vertical surface that moves with the nose of the inviscid SW gravity current is treated as a discontinuity. Following Benjamin (1968), it can be shown that volume and momentum balances about the front, supplemented by the constraint that the energy in this domain cannot increase, require that the velocity of

propagation must be connected with the height of the current at the front by

$$u_N = \left(\frac{|\Delta\rho|}{\rho_a} g \right)^{1/2} h_N^{1/2} \, Fr(a), \quad \text{and} \quad a \leqslant \frac{1}{2}, \tag{2.6}$$

where N denotes the nose (front), $a = h_N/H$ and $Fr(a)$ is Benjamin's Froude number function:

$$Fr(a) = [(2-a)(1-a)/(1+a)]^{1/2}. \tag{2.7}$$

The effect of the curvature terms on the front boundary condition, which is of the order of magnitude of h_0/r_0, was neglected; this is consistent with the previous SW simplifications.

We emphasize that (2.1) and (2.3)–(2.7) are applicable to both heavy and light currents (this is the reason for using the absolute value of $\Delta\rho$). The non-Boussinesq effect is already evident: (2.6) indicates that the speed of the front is proportional to $|\Delta\rho|/\rho_a$, while according to (2.3) and (2.4) the intrinsic speed of the current is proportional to $|\Delta\rho|/\rho_c$. This apparent conflict is accommodated by the thickness (representing the pressure distribution) that thus becomes a function of ρ_c/ρ_a. This interplay between speed and height is the backbone of the model. Estimates of the effect of the return flow suggest that the momentum balance (2.3) is restricted to, roughly, $H^*(\rho_c/\rho_a) > 2$, but there are indications that the model is useful beyond this bound (U; Bonometti *et al.* 2008; Bonometti & Balachandar 2009). The other two equations of the model, (2.1) and (2.6), have a wider range of relevance and thus restrain the global error.

3. Results

3.1. *Numerical solutions to the SW equations*

The gravity current in two-dimensional rectangular geometry displays a constant-speed propagation during the initial slumping stage. In this case, the constant speed u_N and height h_N can be obtained by simple analytical methods as summarized by U. The axisymmetric current is, in general, different.

Consider the characteristic equations (2.4) and (2.5). The axisymmetric system contains a non-zero term on the right-hand side of (2.4), whose contribution is zero at $t = 0$, but develops with time (on a forward-propagating characteristic, the value is negative). Therefore, the axisymmetric current starts with the same u_N and h_N as the rectangular current, but, in general, the subsequent values of these variables will decrease. This is the effect of the diverging geometry, which is relevant to both Boussinesq and non-Boussinesq currents.

There is an exception: when $H^* < 2$ and ρ_c/ρ_a is sufficiently small, the initial u_N is determined by the energy limitation $h_N = H/2$. As long as this limitation must be enforced on the axisymmetric current, it propagates with the appropriate constant speed. However, even these exceptional circumstances are relaxed after a small distance of propagation, Δr. We estimate this distance of restricted (choked) conditions using the forward characteristic in (2.4), with the initial conditions $h \approx h_0$, $r \approx r_0$ and the increments $\Delta h = h_0 - H/2$, $\Delta r \approx u\Delta t$, $\Delta u = 0$. We obtain

$$\frac{\Delta r}{r_0} \approx 1 - \frac{1}{2} H^*, \quad (H^* \leqslant 2). \tag{3.1}$$

This estimate was confirmed by finite-difference solutions to the SW equations. The main conclusion is that the energy-restricted half-depth current is a minor occurrence in the axisymmetric geometry. This is in contrast with the rectangular geometry,
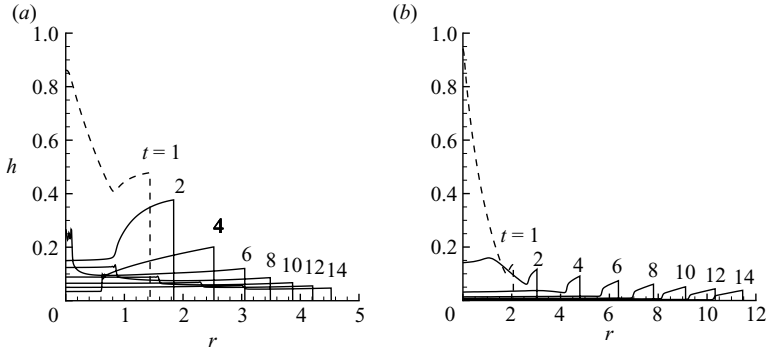
FIGURE 2. Thickness profiles for various t of (a) light $\rho_c/\rho_a = 0.25$ and (b) heavy $\rho_c/\rho_a = 4$ axisymmetric currents released from rest. $H^* = 4$. Finite-difference solutions to the SW equations.
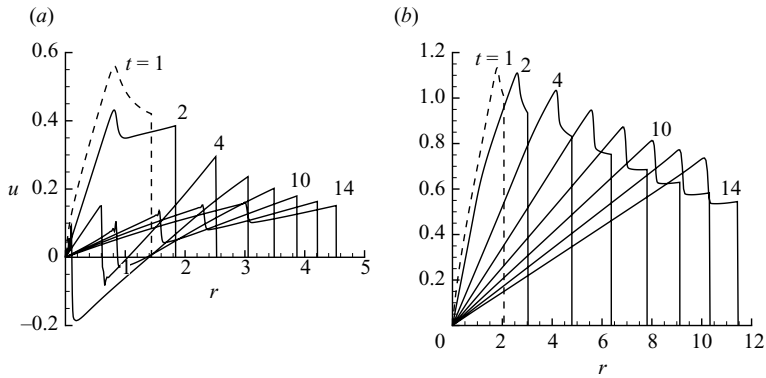

FIGURE 3. Velocity profiles of the currents above.

where the half-depth restriction plays a major role in the propagation of currents with $\rho_c/\rho_a < 1.4$ (approximately) and $H^* < 2$ (Birman, Martin & Meiburg 2005; Lowe *et al.* 2005; U).

The SW equations (2.1) and (2.3), subject to (2.6), $u(r = 0, t) = 0$, and realistic initial conditions for h and u, must, in general, be solved numerically. However, the computational effort (by Lax–Wendroff or similar method for a hyperbolic system) is insignificant. Here, we present finite-difference solutions obtained by a Lax–Wendroff scheme on grids with 500 intervals over $0 \leqslant r \leqslant r_N$.

Hereafter, we scale r by r_0; h, z by h_0; u by $u_{ref} = (|\Delta\rho|gh_0/\rho_c)^{1/2}$; and t by r_0/u_{ref}.

Typical solutions to a light $\rho_c/\rho_a = 0.25$ and heavy $\rho_c/\rho_a = 4$ current, both with $H^* = 4$, are displayed in figures 2 and 3. (The two-dimensional counterpart of figure 2 is shown in figure 3 of U.) For comparison, the solution to the Boussinesq axisymmetric case is given in figure 4.

The SW solutions show significant differences between the light and heavy currents. The heavy current propagates faster, and after a while most of the volume is concentrated in a narrow ring (torus) following the rim $r_N(t)$. The light current propagates slower and tends to develop a more-or-less r-independent thickness.

These different behaviours at large times are well described analytically as follows.
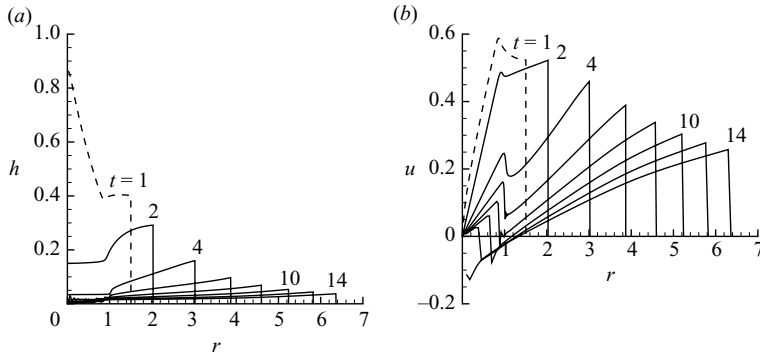
FIGURE 4. The h and u profiles for various t of Boussinesq $\rho_c/\rho_a = 1$ axisymmetric current. $H^* = 4$. (The SW equations in scaled form are the same as those for the non-Boussinesq cases.)

3.2. *Self-similar stage*

After a significant propagation, the current 'forgets' the initial conditions and a self-similar behaviour is expected. Now the current is sufficiently thin (or deep) so that the Fr at the front becomes constant. We define

$$\mathscr{F}^2 = \frac{\rho_c}{\rho_a} Fr^2(0) = 2\frac{\rho_c}{\rho_a}. \qquad (3.2)$$

We use dimensionless variables as defined above. The exact solution to (2.1), (2.3) and nose boundary conditions is now

$$r_N(t) = At^{1/2}, \quad u = \dot{r}_N y, \quad h = \dot{r}_N^2 \frac{1}{2}(y^2 + c), \qquad (3.3)$$

where

$$y = \frac{r}{r_N}, \quad c = \frac{2}{\mathscr{F}^2} - 1 = \frac{\rho_a}{\rho_c} - 1; \qquad (3.4)$$

the over dot denotes the time derivative and A is a constant. These results were also derived by Fanneløp & Jacobsen (1984), but with an unspecified value of $Fr(0)$.

Both light and heavy currents propagate with $t^{1/2}$. There is, however, a difference in the expected shape. For very light currents the small $\mathscr{F}$ produces $c \gg 1$, and hence the profile is a spreading cylinder, $h \approx (A^2/8)ct^{-1}$, with a relatively small contribution from the y^2 term. The opposite structure of a sharp tail-to-head difference is expected for the very heavy current as follows.

First, we note that c decreases when $\mathscr{F}$ increases. For $\rho_c/\rho_a > 1$, we obtain negative values of c, and hence in this case h predicted by (3.3) is negative for $y < y_1$, where

$$y_1 = (1 - \rho_a/\rho_c)^{1/2}. \qquad (3.5)$$

This possible peculiar negative h has been reported by Fanneløp & Jacobsen (1984) and Gratton & Vigo (1994) for a self-similar heavy current (however, with an unspecified value $Fr(0)$, which left the position y_1 undetermined; here we use the specific (3.2) and obtain the clear-cut (3.5)). These previous studies suggested that the negative h of the similarity result means that the heavy current leaves behind a bare bottom, or an empty spot, in the region $y < y_1 At^{1/2}$, approximately. However, the evolvement of this peculiar shape for a realistic current released from behind a lock needs clarification.

We observe that the region where the classic similarity result (3.3) yields a negative h is actually covered by a thin horizontal tail of the current. This corresponds to another branch of the long-time exact solutions to the SW equations (2.1) and (2.3), namely

$$h(r, t) = C/t^2, \quad u(r, t) = r/t, \tag{3.6}$$

where C is a constant of the order unity. The numerical SW results indicate that this solution develops for small r during the transition from slumping to similarity phases. For a heavy current this inner-solution branch spreads out and prevails for large times because it is able to coexist with the fast-moving nose. (For a Boussinesq and light current this inner domain is pushed back by fluid hindered by the slow nose, see the negative u in figures 3a and 4, and then disappears. More details on this quite slow process can be found in Ungarish 2009, §§ 6.3 and 16.3.3.1.)

The self-similar flow for $\rho_c/\rho_a > 1$ combines the horizontal 'tail' (3.6) for $0 \leqslant y < y_m$ and the prominent head (3.3) for $y_m \leqslant y \leqslant 1$, where $y_m \approx y_1$. The volume of the fluid in the tail decays like t^{-1}, which justifies the simplification of a bare bottom left behind a very heavy current. The appearance of such a structure is consistent with the observations during the Thorney Island experimental release of heavy gas in the atmosphere (see figure 6.7 in Simpson 1997), but reliable data for comparisons are unavailable; moreover, viscous effects are expected to affect the decay of the thin tail. We note in passing that the Boussinesq axisymmetric current also displays, for a while, a ring–tail profile (i.e. most of the volume is in a ring that follows r_N). However, this is a transient stage of the Boussinesq current; eventually, the volume flows back from the ring into the tail (see the negative u in figure 4), and the self-similar solution has no bare spot.

Finally, the constant A follows from the volume conservation in the y domain $[y_j, 1]$, where $y_j = 0$ for $\rho_c/\rho_a \leqslant 1$, or y_1 for a heavier current. This yields

$$A = \begin{cases} 2 \left(2\dfrac{\rho_a}{\rho_c} - 1 \right)^{-1/4}, & (\rho_a/\rho_c > 1), \\[4mm] 2 \left[2\dfrac{\rho_a}{\rho_c} - 1 + \left(\dfrac{\rho_a}{\rho_c} - 1 \right)^2 \right]^{-1/4}, & (\rho_a/\rho_c \leqslant 1). \end{cases} \tag{3.7}$$

The self-similar analytical results describe well the main features displayed by the numerical solution to the SW equations for large t. However, the formulas (3.3) are not a complete prediction tool because initial conditions are not satisfied, and t can be replaced by $t + \gamma$. For practical use of the self-similar results, the constant γ must be determined by matching with another solution or experiment, which accounts for the initial conditions.

3.3. *Navier–Stokes support*

Some NS simulations were carried out to gain support for the SW results. We used an axisymmetric finite-difference code of the type described by Ungarish & Huppert (2004). As pointed out above, the Boussinesq axisymmetric simulations become unreliable for $r_N > 2.5$ (approximately). We found that the non-Boussinesq cases are prone to a similar instability (actually, more pronounced when $|\rho_c/\rho_a - 1|$ increases).

The results shown in figures 5 and 6 are for $\rho_c/\rho_a = 1/2$ and 2, with $H^* = 2$. (Note that here the parameters are different from those of figure 2, because the latter would have required significantly more CPU, storage and processing resources.) The NS runs were performed for a container of radius 4.5, $h_0/r_0 = 0.5$, free-slip boundaries,
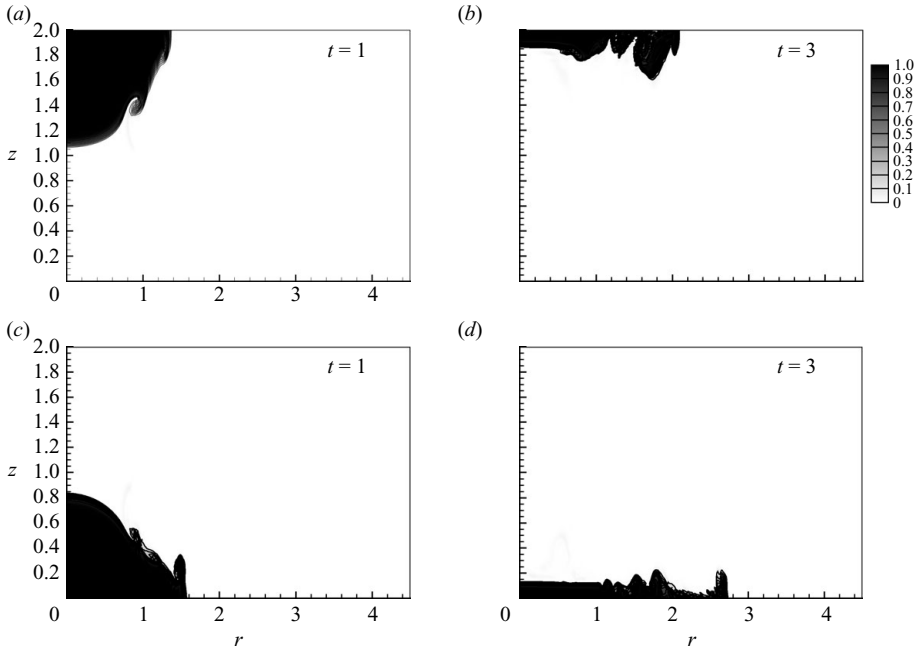
FIGURE 5. NS results (density function contours) for currents with $H^* = 2$ at times $t = 1$ and 3. (*a,b*) Light current with $\rho_c/\rho_a = 1/2$. (*c,d*) Heavy current with $\rho_c/\rho_a = 2$.
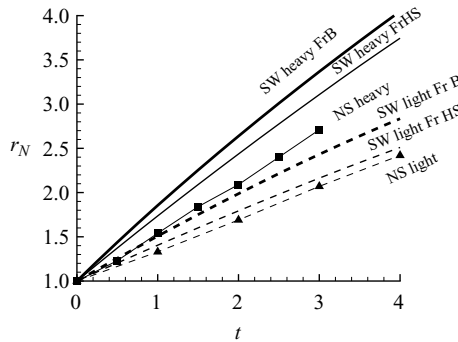

FIGURE 6. r_N as a function of t for light $\rho_c/\rho_a = 0.5$ and heavy $\rho_c/\rho_a = 2$ currents; $H^* = 2$. NS (symbols joined by thin lines) and SW (lines) for Benjamin's and Huppert–Simpson Fr, results.

$Re = 1.8 \times 10^4$ and 400×200 grid (stretched in z to increase the resolution of the current). The density function varies from zero in the ambient to one in the pure current, and the diffusion term added in the density transport equation to smooth out the jump at the interface corresponds to a Schmidt number of about 10; this artificial term is insignificant for the times discussed here; see Bonometti & Balachandar (2008). Various verification runs with changes of grid, time step and other parameters were also performed. Note that in the frames of figure 5 the z/r axis ratio is stretched; for estimating the 'real' appearance of the currents, we must recall the z/h_0, r/r_0 scaling, and that $h_0/r_0 = 0.5$. The complex NS interface is only roughly reproduced by the SW smooth $h(r, t)$. This discrepancy also appears in Boussinesq cases (see Ungarish 2007*a*).

These simulations confirm the SW differences between the heavy and light currents, but cannot be used to verify the self-similar propagation (expected for large r_N), because unphysical instabilities appear for $r_N > 2.5$. Consider the details of r_N as a function of t given in figure 6. The NS results (the symbols in the figure) show that light current with $\rho_c/\rho_a = 1/2$ propagates slower than the heavy current with $\rho_c/\rho_a = 2$. The agreement with the SW results is fair. The discrepancies can be attributed to a combination of deviations from the idealized SW conditions. First, it could be expected that SW results based on Benjamin's Fr exaggerate the speed of propagation. SW results with the Huppert–Simpson Fr (see Ungarish 2009) are also shown in figure 6, and indeed improve the agreement; this trend for the two-dimensional counterpart was shown by Bonometti & Balachandar (2009). In addition, the real flow is affected by an initial adjustment stage (during which the SW assumption of a small height to length ratio of the flow domain is not satisfied), shear and mixing at the interface and the appearance of the above-mentioned instability; these hindering effects are not taken into account by the SW approximations. We see that the NS current shows a non-physical tendency to accelerate at $t \approx 3$; this illustrates the limitation of the simulations. For more accurate and longer time comparisons, it is necessary to employ more sophisticated and three-dimensional NS codes and powerful computers; this is a major project beyond our objective.

4. Concluding remarks

We presented a compact SW model for the high-Reynolds axisymmetric gravity current that covers a quite wide parameter range of density ratio of current to ambient fluids, ρ_c/ρ_a, and of the depth ratio H^*, and contains no adjustable constants. This set of hyperbolic equations for the thickness $h(r, t)$ and speed $u(r, t)$ must be solved, in general, numerically–but this requires insignificant computer time. For large times a self-similar behaviour, which can be described analytically, appears; however, for practical applications this result must be matched with numerical or experimental data that contain the appropriate initial conditions. The Boussinesq currents are now a narrow strip about $\rho_c/\rho_a = 1$ in the wide parameters domain $(H^*, \rho_c/\rho_a)$ covered by the model.

The main differences between the axisymmetric light and heavy currents, and between the two-dimensional (rectangular) counterparts, were elucidated.

We showed that the SW results are consistent with NS axisymmetric simulations. However, the axisymmetric codes seem unable to reproduce realistic propagations beyond $r_N \approx 3$ (scaled with the initial r_0). A comprehensive assessment of the SW model requires three-dimensional NS simulations and/or dedicated experiments, which are presently unavailable. We hope that this paper will provide the motivation and guiding lines for these investigations. An interesting and useful feature of the Boussinesq SW model is that it remains a reliable prediction tool beyond the r_N where the NS axisymmetric simulations fail. We expect that this important property carries over to the non-Boussinesq case.

The suggested theory is a potentially advantageous tool for the understanding and modelling of the axisymmetric gravity current; but we must keep in mind that further tests are necessary for a clear-cut determination of the range of validity and accuracy of the results. The present model is expected to be a useful extension of the corresponding two-dimensional counterpart, because radial–cylindrical propagation is relevant in practical natural and hazard-prediction problems. The fact that Boussinesq and non-Boussinesq light and heavy currents can now be treated in a unified form by a

single simple formulation is expected to promote the investigation of non-Boussinesq cases. This model is amenable to extensions to more complex circumstances, in particular to rotating systems.

REFERENCES

BENJAMIN, T. B. 1968 Gravity currents and related phenomena. *J. Fluid Mech.* **31**, 209–248.

BIRMAN, V. K., MARTIN, J. E. & MEIBURG, E. 2005 The non-Boussinesq lock exchange problem. Part 2: High-resolution simulations. *J. Fluid Mech.* **537**, 125–144.

BONOMETTI, T. & BALACHANDAR, S. 2008 Effect of Schmidt number on the structure and propagation of density currents. *Theor. Comput. Fluid Dyn.* **22**, 341–361.

BONOMETTI, T. & BALACHANDAR, S. 2009 Slumping of non-Boussinesq gravity currents of various initial fractional depths: a comparison between direct numerical simulations and a recent shallow-water model. *Computers and Fluids,* doi:10.1016/j.compfluid.2009.11.008.

BONOMETTI, T., BALACHANDAR, S. & MAGNAUDET, J. 2008 Wall effects in non-Boussinesq density currents. *J. Fluid Mech.* **616**, 445–475.

CANTERO, M., BALACHANDAR, S. & GARCIA, M. H. 2007 High resolution simulations of cylindrical density currents. *J. Fluid Mech.* **590**, 437–469.

FANNELØP, T. K. & JACOBSEN, Ø. 1984 Gravity spreading of heavy clouds instantaneously released. *ZAMP* **35**, 559–584.

GRATTON, J. & VIGO, C. 1994 Self-similar gravity currents with variable inflow revisited: plane currents. *J. Fluid Mech.* **258**, 77–104.

KELLER, J. J. & CHYOU, Y.-P. 1991 On the hydraulic lock-exchange problem. *ZAMP* **42**, 874–910.

LOWE, R. J., ROTTMAN, J. W. & LINDEN, P. F. 2005 The non-Boussinesq lock exchange problem. Part 1: Theory and experiments. *J. Fluid Mech.* **537**, 101–124.

PATTERSON, M. D., SIMPSON, J. E., DALZIEL, S. B. & VAN HEIJST, G. J. F. 2006 Vortical motion in the head of an axisymmetric gravity current. *Phys. Fluids* **18**, 046601(1–7).

SIMPSON, J. E. 1997 *Gravity Currents in the Environment and the Laboratory*. Cambridge University Press.

UNGARISH, M. 2007a Axisymmetric gravity currents at high Reynolds number: on the quality of shallow-water modelling of experimental observations. *Phys. Fluids* **19**, 036602/7.

UNGARISH, M. 2007b A shallow water model for high-Reynolds gravity currents for a wide range of density differences and fractional depths. *J. Fluid Mech.* **579**, 373–382 (referred to as U).

UNGARISH, M. 2009 *An Introduction to Gravity Currents and Intrusions*. Chapman & Hall.

UNGARISH, M. & HUPPERT, H. E. 2004 On gravity currents propagating at the base of a stratified ambient: effects of geometrical constraints and rotation. *J. Fluid Mech.* **521**, 69–104.